Notch Sensitivity of Aliphatic Polyketone Terpolymers

W. C. J. Zuiderduin, J. Huétink, R. J. Gaymans

Department of Chemical Technology, University of Twente, P.O. Box 217, 7500 AE Enschede, The Netherlands

Received 18 December 2002; accepted 27 June 2003

ABSTRACT: The notch sensitivity of aliphatic polyketone (PK) terpolymers was investigated in this article. The notch-tip radius was varied between the size of an actual propagating crack tip of 1–2 μm and the largest notch tip of 1000 μm radius. The larger notch-tip radii (1000–15 μm) were milled into the polymer. The smallest notch-tip radii of 2 and 15 microns were made with a novel technique with the aid of an Eximer laser. The fracture behavior of the PK–terpolymer was found to be sensitive toward changes in notch-tip radius. The fracture energy decreased strongly with decreasing notch-tip radius even when fractured ductile. Sharper notches were not as effectively blunted as were larger notches in the ductile region. The brittle-to-ductile transition temperature (T_{bd}) was increased with decreasing notch-tip radius for the larger notches (1000–100 μm). For sharper notches (2 and 15 μm) the T_{bd} decreased again. This behavior could be explained by the decreasing amount of elastic energy release with sharper notches. The energy release proved to be very important for this material. A mixed-mode fracture behavior was found to occur with larger notches because of the elastic energy present in the sample before fracture. The notch sensitivity was reduced considerably by the addition of a 10% core–shell rubber phase. For the blend material the notch-tip radius had almost no influence on the T_{bd}. The fracture energy on the other hand was still lowered with a sharper notch. This was attributed to the difference in the crack initiation process. © 2003 Wiley Periodicals, Inc. J Appl Polym Sci 91: 2558–2575, 2004

Key words: impact resistance; mechanical properties; toughness; fracture; core–shell polymers

INTRODUCTION

Unnotched samples of semicrystalline polymers often fracture in a ductile manner. However, with a notch or defect they nearly all show brittle fracture. In many polymers the change from craze formation to large-scale yielding at the crack tip is the mechanism responsible for the observed brittle-to-ductile transition. Conditions that promote shear yielding at the expense of crazing include elevated test temperatures,[1–4] decreasing section thickness, decreasing strain rate, absence of an aggressive environment, and certain features of the polymer's chemical and physical structure. The transition from brittle to ductile behavior has been explained by a competition between shear yielding and a crazing mechanism[5–7] and sometimes appears to involve a mixed-mode transition.[2,8,9]

Polymers are said to be notch sensitive. It is well known that sharper notches lower the fracture energy. The effects of a sharper notch are: (1) a higher stress concentration at the notch tip; (2) a higher local strain rate at the notch tip; (3) an enhanced plane strain field at the notch tip. This latter property suppresses shear yielding mechanisms of the polymer.[10–14]

Correspondence to: R. J. Gayman (R.J.Gaymans@ct.utwente.nl).

Journal of Applied Polymer Science, Vol. 91, 2558–2575 (2004)

It is expected that with a sharper notch the energy necessary to fracture the specimen decreases considerably and the brittle-to-ductile transition temperature will be lowered.

Stress concentration

Sharp notches result in a certain stress concentration factor behind the notch. The most simple case is an elliptical hole in a sheet, with mean axis A and secondary axis B and radius of curvature ρ. Williams described the influence of radius of curvature on the stresses around an elliptical hole in a material with[14]

$$\sigma_{yy} = \sigma\left(1 + 2\sqrt{\frac{A}{\rho}}\right) \tag{1}$$

where σ_{yy} is the stress in the y-direction at $x = A$, the radius of curvature $\rho = B^2/A$ at the tip of the elliptical hole, and σ is the remote stress. This equation can be used to estimate the stress concentration for notches that can be approximated by an ellipse. For a circular hole, $\rho = A$ and $\sigma_{yy} = 3\sigma$.

For a crack, $B \ll A$, this model results in infinite stress at the crack tip. This concept is used in many different notch configurations. In more complex systems, numerical solutions are used; one example is the Neuber equation[15]:

$$K_{tn} = 1 + \sqrt{\frac{(K_{te} - 1)^2(K_{th} - 1)^2}{(K_{te} - 1)^2 + (K_{th} - 1)^2}} \tag{2}$$

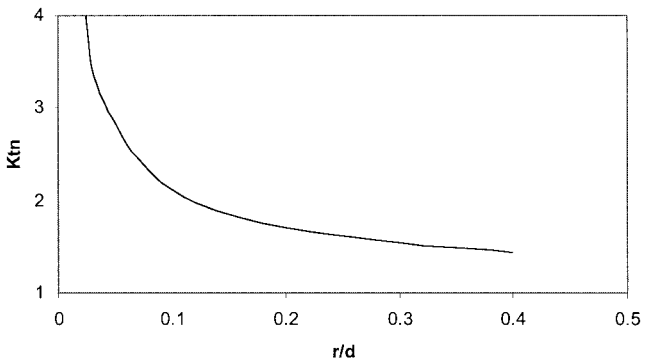

Figure 1 Stress–concentration factors for single-edge V-notch in tension in a semi-infinite specimen.[15]

where K_{te} is the stress concentration factor for a shallow elliptical notch in a semi-infinite wide specimen and K_{th} is the stress concentration factor for a deep hyperbolic notch in an infinitely wide specimen. For this specific case of a single-edge V-notch in tension in a semi-infinite specimen, the result for the stress concentrations are shown in Figure 1.

In a standard Izod test the notch-tip radius $r = 0.25$ mm and ligament behind the notch $d = 8$ mm. This results in a K_{tn} value of 3.34. This plot also predicts very large stress concentrations at very sharp notches and even infinite for a realistic crack tip.

Fracture toughness

Using fracture toughness parameter G, it was deduced that a linear relationship exists between the blunt-notch strain energy release rate G_B and notch-tip radius (ρ)[14,16]:

$$\frac{G_B}{G_C} = \frac{1}{2} + \frac{\rho}{8l_0} \tag{3}$$

where G_C is the value for a sharp notch, l_0 is the distance ahead of the notch tip at which the stress reaches a critical level and fracture occurs, and $\rho \gg l_0$. This linear relationship was confirmed by experimental results for poly(vinyl chloride).[17]

The method for determination of G_B is applicable only when crack initiation is followed by unstable brittle fracture with no further energy absorption (thus for rather brittle materials). When blunting occurs at the crack tip, the constraint ahead of the tip is reduced and this influences the measured toughness. The effect of notch radius on K_{Ic} was described by Kinloch[1,18] and others.[8] They also found that an increase in notch radius resulted in higher fracture stress and thus higher toughness.

The effect of notch radius on the fracture of polymers was the focus of a number of studies.[5,8,13,19,20] Many practical impact tests have been carried out on specimens with notches of finite tip radius because these notches are more easily reproduced. Standard ASTM specimens have a notch-tip radius of 0.25 mm. Sharp notches are usually obtained by pushing a razor blade in the material and, with this method, tip radii on the order of 10 μm or less can be obtained.[16] The razor procedure, however, results in plastic deformation in the material around the crack tip zone before actual testing and this can influence the test results.

Polato[21] studied poly(butylene terephthalate) containing a standard notch in a Charpy test and found that the strain rate at the notch root was 2300 s^{-1}, which is very high. In notched Izod strain rate at the notch tip was estimated to be in the order of 5000 s^{-1}.[22] This indicates the extent that a notch concentrates stress and strain at the notch tip.[20]

The dependency of the yield stress on strain rate for polymers has been studied on several occasions, where it was found that the yield stress increases with strain rate. A smaller notch radius will therefore cause an increase in yield stress and thus eventually leads to a transition from ductile to brittle behavior.[19]

Pitman and coworkers[5] used different notch-tip radii in their study on impact behavior of PC, as did Fraser and Ward.[19] PC specimens fractured in a brittle manner for small radii, and ductile for very blunt notches. In between these two extremes a region has been found where three types of fracture are observed: brittle, brittle with small yielded zones, and completely ductile. This is associated with the transition from plane strain (sharp notch) to plane stress (blunt notch). Similar behavior was found by Havriliak et al.,[20] who also stated that changing the notch-tip radius directly affected the strain rate at the tip. Notch radii used in the above-mentioned surveys, however, are usually quite large compared to the radius of a hairline crack attributed to ageing, a craze, or a running crack in the material. In such cases the notch-tip radius is in the order of 1 μm.[23] The influence of rubber addition to polymers in this context has rarely been studied. Here, the effect of notch radius on fracture stress and energy is studied as a function of temperature. The change of brittle-to-ductile transition temperature is also investigated.

A generally accepted method for investigating notch sensitivity is the standard Izod impact test. In literature the notch-tip radii are usually varied from 0.25 mm to much larger values (Fig. 2).

Sometimes the razor-blade method is used to produce sharp notches, but with this method it is difficult to reproduce and to control the actual size of the notch tip. Therefore it was decided that sharp notches would be produced with a novel laser technique. Sharp notches are interesting because it may be possible to approach the size of a tip of an actual running crack. An arrested crack in polyketone rubber blend was isolated and microtomed with a diamond knife; after

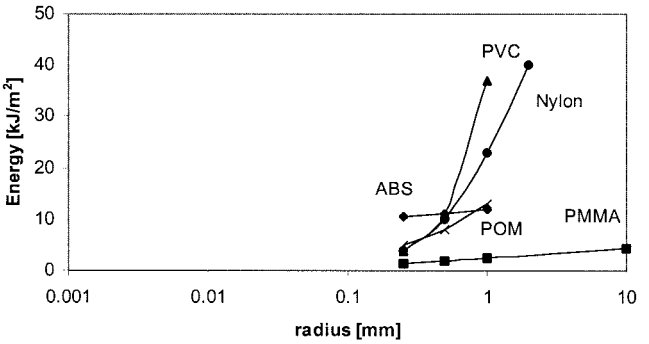

Figure 2 Impact energy as a function of notch-tip radius for some engineering polymers.

being coated with a gold layer the sample was studied by scanning electron microscopy (SEM), the results of which are shown in Figure 3.

The actual crack tip has a radius of about 1 micron; this is 3 orders of magnitude smaller than the standard notch in an Izod or Charpy test. This crack is not strained; it should be noted that a crack tip under strain could have a somewhat different size; moreover, the crack tip may have been ameliorated to some extent.

Aim

The experiments conducted in this study were performed to investigate the influence of notch-tip radius on the fracture behavior of an aliphatic polyketone terpolymer (PK) and a blend of PK–terpolymer with 10% of a core–shell rubber phase (PK_{90}–CSR_{10}). The notch-tip radius was varied from a relatively large radius (1000 μm) to very sharp notches (2 μm). The standard notch used in Izod and Charpy tests is 250 μm. The ligament behind the notch tip was kept constant at 8 mm. The different specimens were tested in a single-edge notched tensile (SENT) setup. The temperature was varied to obtain complete brittle and complete ductile fracture.

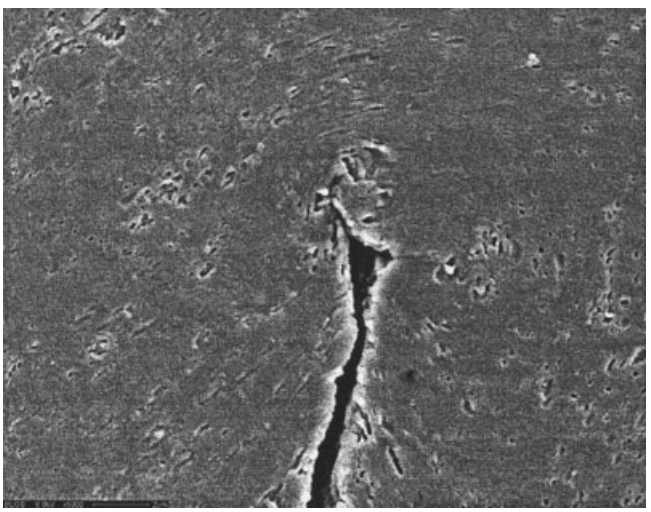

Figure 3 SEM image of arrested crack in aliphatic polyketone–rubber blend.

TABLE I
Material Specifications

Material	Produced by	Description
Carilon P1000	Shell	Polyketone terpolymer with 6 mol % propylene. Density 1.24 g/cm^3. T_m = 225°C, T_g = 15°
Blendex 338	GE plastics	Core–shell rubber, PB core with a SAN shell particle size: 200 nm

EXPERIMENTAL

Materials

Commercially available polyketone and blendex core–shell rubber were kindly supplied by Shell (Amsterdam, The Netherlands) and GE Plastics (Bergen op Zoom, The Netherlands). Material specifications are listed in Table I.

The polyketone used in this study is a perfect alternating terpolymer, polymerized from ethylene and carbon monoxide; 6 mol % of the ethylene was replaced by propylene to lower the melting temperature. This polyketone has a glass-transition temperature of about 15°C and a melting temperature of 225°C with a crystallinity of 35 wt %.

Specimen preparation

Compounding of the materials was done using a Berstorff (ZE 25 × 33D) twin-screw extruder (Hanover, Germany). In the extrusion step, barrel temperatures were set at 225/240/240/240/240/240/240°C and a screw speed of 140 rpm. During the extrusion process stabilizers were added, 0.2 wt % calcium–hydroxyl–apatite (melt stabilization), 0.3 wt % Nucrel (ethylene–methacrylic acid copolymer, processing aid), and 0.2 wt % Naugard [2–2′-oxamidobis(ethyl-3(3,5 di-*t*-butyl-4-hydroxyphenyl)propionate)], antioxidant.

After compounding, the blend and the polyketone terpolymer were injection molded into rectangular bars of 74 × 10 × 4 mm using an Arburg Allrounder 221-55-250 injection-molding machine (Losburg, Germany). The barrel had a flat temperature profile of 240°C, and the mold temperature was kept at 70°C with an injection pressure of 55 bar; the holding pressure was kept at 45 bar.

Conditioning

The test bars were dried at 80°C under vacuum for 15 h, and kept under vacuum at room temperature

TABLE II
Infrared Camera Specifications

TVS 600 AVIO Nippon Avionics Co.	
Temperature range	−20 to 300°C
Temperature resolution	0.15°C
Spectral range	8–14 μm
Image rate	30 frames/s
Spatial resolution	0.1-mm spot size

after this drying step. Because of the physical ageing behavior of this type of polyketone, every 10 days the test bars were heated to 80°C for 0.5 h to rejuvenate the physical ageing. After this treatment the test bars were cooled in a controlled manner in the oven and kept under vacuum. The test bars were not used in the first 2 days after a heat treatment because the physical ageing process is very fast in this period.

Notched Izod impact test

Notched Izod impact tests were carried out using a Zwick pendulum (Ulm, Germany). To vary the test temperature, the specimens were placed in a thermostatic bath. The impact strength was calculated by dividing the absorbed energy by the initial cross-sectional area behind the notch (32 mm^2). All measurements were carried out 10 times.

SEM micrography

SEM micrographs were taken to study the effect of thickness on the final morphology of the materials. Samples were taken from the core of the injection-molded bars. SEM specimens were prepared by cutting with a CryoNova microtome at −110°C using a diamond knife (−100°C) and a cutting speed of 1 mm/s. The cut surfaces were then sputter-coated with a thin gold layer and studied with Hitachi S-800 field emission SEM (Hitachi, Ibaraki, Japan).

Infrared thermography

The temperature increase during fracture of specimens containing notches of radii 0.002–1 mm was monitored using an infrared camera. Specifications are listed in Table II. With the infrared camera, only temperatures at the surface of the specimen can be determined. Temperatures inside the specimen are expected to be higher than those at the surface. The spot size of about 100 μm is relatively large. The temperature indicated in one spot is an average temperature over the entire spot size. The temperature directly at the fracture surface, which is expected to be highest, thus cannot be determined. The maximum temperature that will be determined from the infrared images is thus not the maximum surface temperature.

SENT experiments

The fracture behavior was studied by a tensile test on notched bars, referred to as single-edge notch tensile (SENT) test. Tests were carried out on a Schenck VHS servohydraulic tensile machine (Darmstadt, Germany). With this apparatus it is possible to achieve clamp speeds ranging from 10^{-5} to 12 m/s. The specimen length between the clamps was 35 mm; thus accordingly the macroscopic apparent strain rate varied from 2.8×10^{-4} to 285 s^{-1}. A pickup unit was used to allow the piston to reach the desired test speed before loading the specimen. All moving parts were made of titanium to diminish the effects of inertia. A rubber pad dampened the contact between the pickup unit and the lower clamp to reduce harmonic oscillations.[24] The clamp displacement was assumed to equal the piston displacement, which was measured with a LVDT. The force was measured with a piezo-electric force transducer located between the upper clamp and the crosshead. Force, time, and piston displacements were recorded using a transient recorder with a maximum sample rate of 2 MHz per channel. After completion of the test the results were sent to a computer. The test setup is given schematically in Figure 4.

The tensile machine was equipped with a temperature chamber. The temperature chamber was heated or cooled with a nitrogen flow, which passed a heating unit. The heating unit was driven by an Eurotherm controller. A thermocouple inside the chamber registered the temperature. Calibration was carried out using a specimen with an embedded thermocouple.

Figure 5 gives a typical stress–displacement curve for a ductile fracture obtained by a SENT test. To characterize the fracture process it may be divided into a crack initiation part and a crack propagation part.

The crack initiation stage starts from zero displacement, and crack initiation is assumed to take place at the point of maximum stress. For low strain rates this was verified with the aid of the time records and the onset of crack initiation was optically determined. For low strain rates the onset of crack initiation always coincides with the point of maximum stress. At high strain rates it is not possible to optically check the point of crack initiation but it is assumed that crack initiation occurs at the maximum stress.

The displacement after the maximum load contributes to the crack propagation part of the fracture process. Brittle fracture is characterized by zero propagation displacement and energy. With ductile fracture the propagation displacement contributes significantly to the fracture displacement.

Notch-processing techniques

A single-edge 45° V-shaped notch of 2 mm depth was milled in the specimens; notch radii of 1, 0.5, 0.25, or

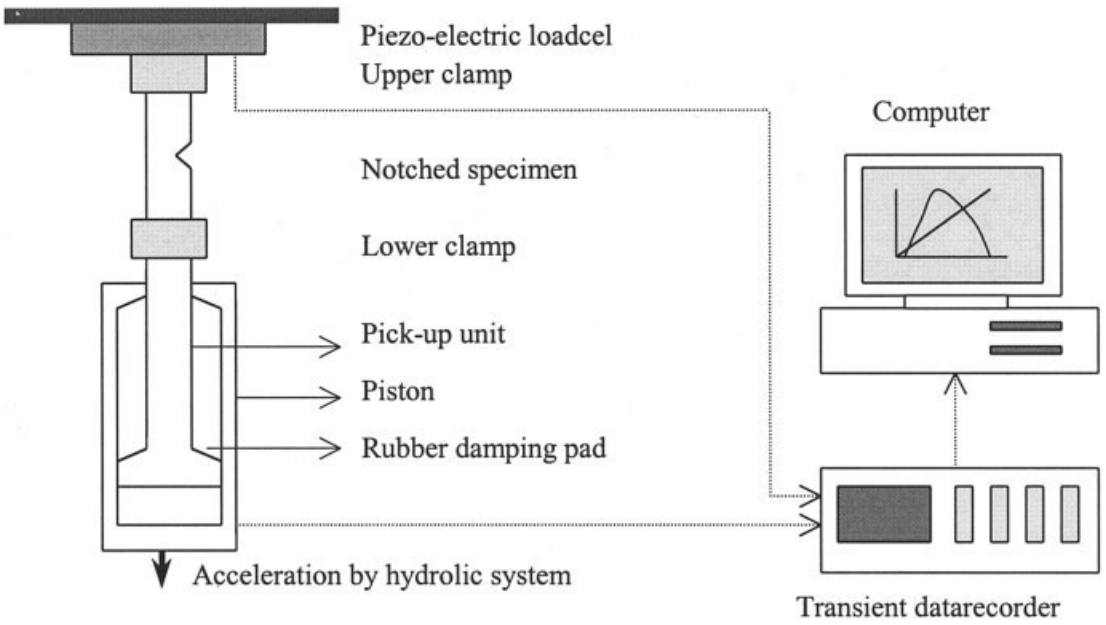

Figure 4 Experimental setup of the Schenck VHS tensile tester.

0.1 mm were possible by using different saws. Using an Excimer laser, 0.1-mm notch radius specimens were then modified by adding a small extra notch at the tip. This resulted in very small notch radii of 0.002 and 0.015 mm. The choice for this type of laser was based on the fact that heat generation in the specimen should be avoided. Melting would reduce the control of notch radius and reproducibility of the notch method. Because of the ablasive process heat generation was kept to a minimum. The laser deploys photogenic charges, which contain the amount of energy to break a covalent carbon–carbon (C—C) bond. The notch-tip radius was varied between the size of an actual propagating crack tip of 1–2 μm and the largest notch tip of 1000-μm radius. The larger notch-tip radii (1000–15 μm) were milled into the polymer. The overlap at 15-μm radius (produced with a cutter and also with laser) was done to observe the effect of the notching method.

To check the radius that was obtained with notching, SEM micrographs were taken from specimens containing the notches produced with the laser technique. The milled-in notches are also shown for comparison. The results of the SEM are shown in Figure 6. (The reader should observe that the magnification varies with notch size.)

The milled notches showed the desired notch radius and a rather clean notch. Treatment with the laser resulted in an additional sharp notch at the original machined notch tip (Fig. 6), and the notch-tip radius of the specimen shown here is close to the average 3-μm radius. The notch-tip radius of 15 μm shown here was made with a cutting technique.

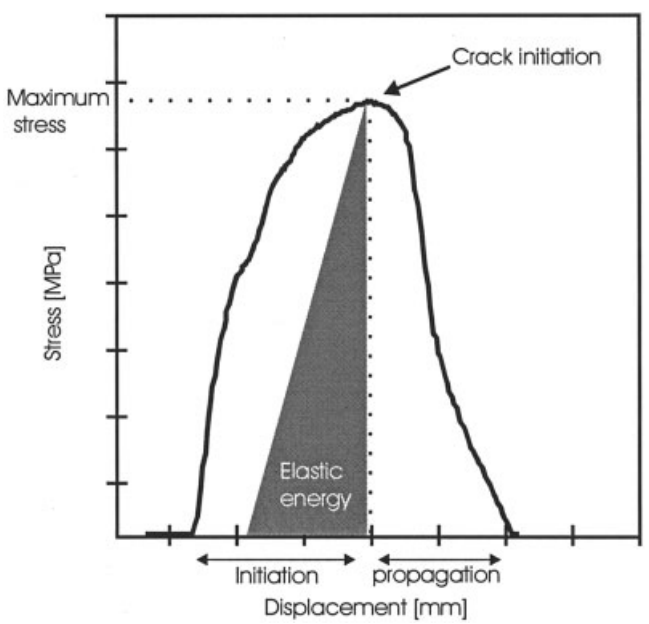

Figure 5 Typical stress–displacement curve obtained by a SENT test.

Parameter definitions

Crack initiation is assumed to occur at maximum load. The point of maximum stress was chosen as the boundary between crack initiation and crack propagation. The following parameters are used to describe the fracture process.

Maximum stress. Maximum force on the force displacement curve, divided by the initial cross-sectional

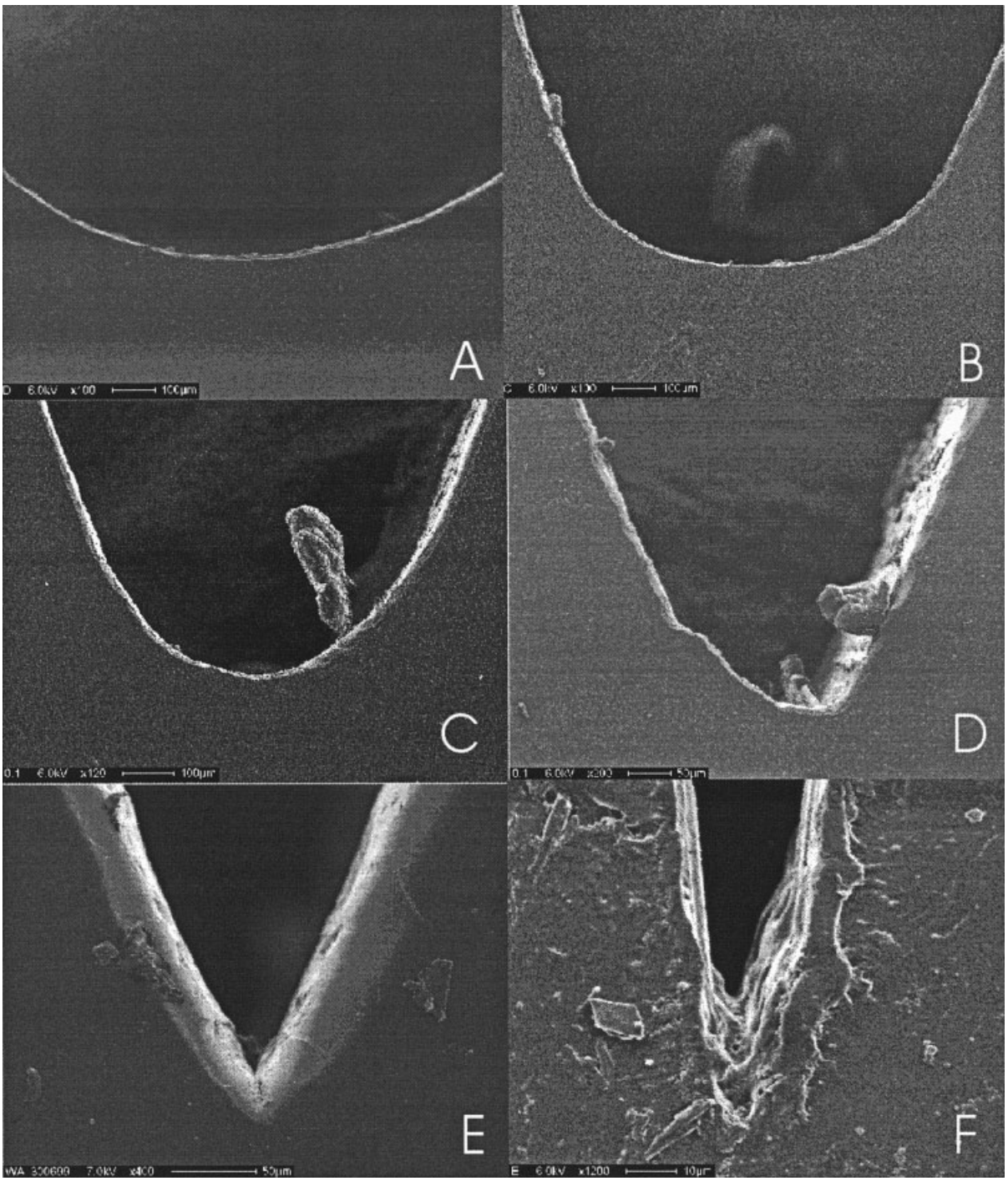

Figure 6 Different notch-tip radii produced in polyketone polymer: (A) 1000 μm; (B) 500 μm; (C) 250 μm; (D) 100 μm; (E) 15 μm; (F) 3 μm.

area behind the notch (32 mm^2). Stress concentrations are neglected.

Initiation displacement. Clamp displacement between the first point of force increase and the point of maximum force.

Initiation energy. Area under the force–displacement curve up to the maximum force.

Crack propagation displacement. Clamp displacement between the point of maximum force and the first point of zero force after decrease in force.

Crack propagation energy. Area under the force–displacement curve after maximum force.

Fracture displacement. Total displacement during the fracture process.

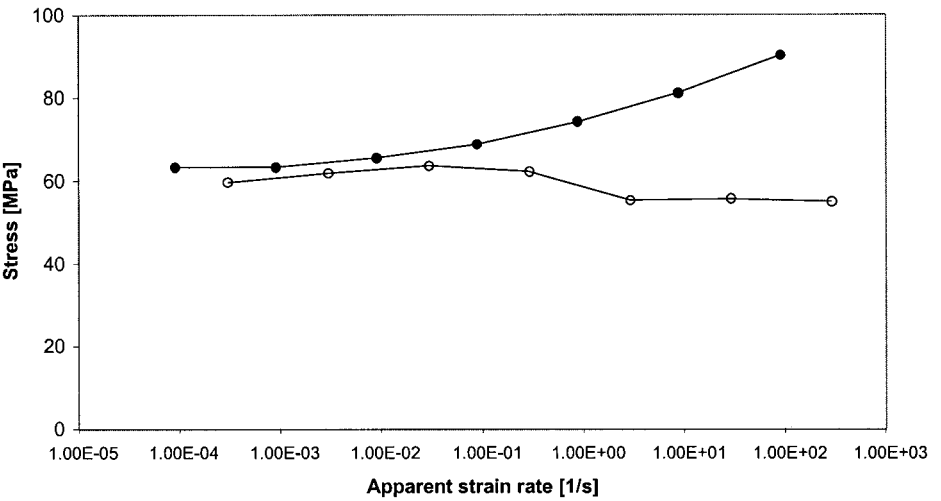

Figure 7 Maximum stress as a function of strain rate for notched and unnotched polyketone, 20°C. ●, Yield stress from unnotched specimen; ○, notched specimen in SENT (radius 0.25 mm, 2 mm depth).

Fracture energy. Total area under the force–displacement curve during the fracture process.

In the case of brittle fracture the force decreases almost instantaneously from the maximum force to zero. Therefore brittle fracture is characterized by a very low propagation displacement and very low propagation energy. The onset of propagation energy and displacement is taken as the marker for ductility. Ductile fracture is defined here as a fracture, which requires additional energy to propagate a crack through the specimen. All measurements were performed five times.

RESULTS AND DISCUSSION

The influence of notch-tip radius on the fracture behavior of an aliphatic polyketone terpolymer (PK) and a blend of PK–terpolymer with 10% of a core–shell rubber phase (PK_{90}–CSR_{10}) was studied. The notch-tip radius was varied from a relatively large radius (1000 μm) to very sharp notches (2 μm). First, the PK terpolymer is discussed and after these results the PK/core–shell rubber blend properties are discussed.

Aliphatic polyketone terpolymer

Tensile behavior

The yield stress of aliphatic polyketone polymer was determined as a function of strain rate. The yield stress was measured on an unnotched dumbbell-shape specimen. For the standard 250-μm notch radius the maximum stress in the SENT test was also measured as a function of strain rate, to compare against the unnotched geometry (Fig. 7).

The apparent strain rate was calculated based on the clamping distance at $t = t_0$; localization effects were ignored. The unnotched specimen reached the yield stress of the aliphatic polyketone polymer, the value given here. These specimens show fully ductile behavior. The yield stress was increased with strain rate. The increase in yield stress was somewhat stronger than expected from the Eyring theory.

The notched specimens showed ductile behavior only at the lowest two strain rates. The notched specimen apparently still showed a lot of plastic deformation behind the notch tip because the stress level reached was close to that of the unnotched specimen. At higher strain rates the stress was lower than that of the notched samples but the stress concentrations seem to be considerably lower than expected from theory. At high strain rates only a stress concentration factor of 1.54 was reached here relative to the unnotched geometry, whereas for this notched geometry the theory predicts[15] a K_{tn} of 3.34. This indicates that, although the macroscopic fracture is brittle, behind the notch tip plastic deformation processes are still locally operative. When the notch is completely blunted by plastic deformation processes, the stress concentration behind the notch tip is diminished, as seems to be the case at low strain rates. Consequently the yield stress of the unnotched geometry is reached. This experiment was performed to illustrate that notch-tip blunting is an important feature of polymers. This behavior was found to be similar to that of polypropylene.[11]

Notched Izod impact

The influences of the notch-tip radius on the impact resistance were studied in two tests, the notched Izod impact test and the SENT test. In a standard notched Izod test the notch-tip radius is 250 μm. The notched

Izod fracture energies as a function of temperature for the different notch-tip radii are given in Figure 8.

The fracture energy increases with temperature for all notch-tip configurations. With the sharpest notches, however, the slope of the lines becomes very shallow.

The impact strength clearly increases with notch-tip radius over the entire temperature range. Upon increasing the notch-tip radius the fracture energy increases by a factor of almost 4. It can be expected that the brittle-to-ductile transition shifts with different notch-tip radii but in this test and within the temperature range used, it is not clear for the polyketone material tested. This is attributed to the fact that fully ductile fractures were not encountered in this temperature range. The effect of radius was quite pronounced (Fig. 8). Figure 9 shows the fracture energy of the PK–polymer as a function of notch-tip radius.

The fracture energy decreased sharply with decreases in the notch-tip radius. The standard notch of 250-μm radius lies in the region where the fracture energy is very sensitive toward changes in notch-tip radius. Thus small changes in notch-tip radius lead to large changes in fracture energy for the polyketone terpolymer when measuring the notched Izod impact strength. The effect of notch-tip radius is also quite large compared to the influence of temperature. With the sharpest notch-tip radii (<100 μm) the energy value converges to approximately 5 kJ/m^2. A sharper notch does not lead to any significantly lower fracture energy in this regime. It is emphasized that the energies shown here are for brittle and semiductile fractures only. No fully ductile fractures were found in this temperature range and only local shear yielding behind the notch tip was observed during these fractures. The notch-tip radius has a significant effect on the impact energy. Notch-tip blunting can be attributed largely to the fracture energy in this polymer especially in the notch-tip radius regime of ≥ 100 μm. When a notched specimen is loaded and local deformation processes blunt the notch, in this regime, the fracture energy will increase sharply, as indicated by Figure 9.

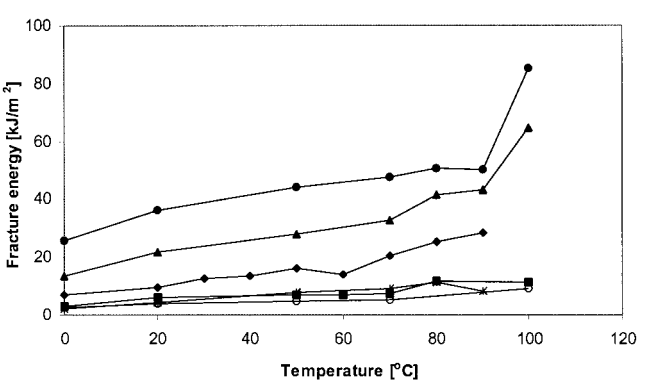

Figure 8 Notched Izod impact results for different notch-tip radii in PK as a function of temperature. Notch-tip radius: ○, 2 μm; *, 15 μm; ■, 100 μm; ◆, 250 μm; ▲, 500 μm; ●, 1000 μm.

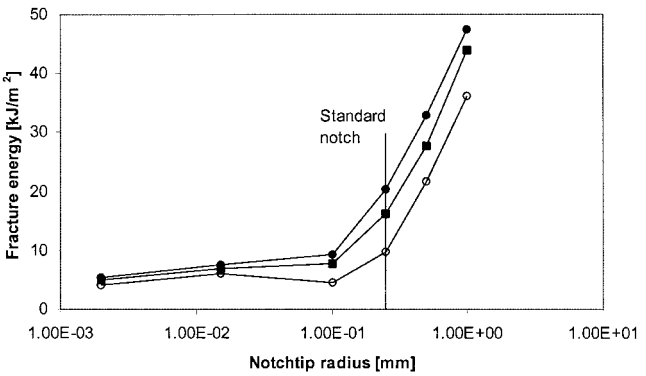

Figure 9 Notched Izod impact results as a function of notch-tip radius for PK–terpolymer: ○, 20°C; ■, 50°C; ●, 70°C.

One problem with the notched Izod impact test is that the specimens are not always broken completely, especially at elevated temperatures where the modulus is lowered and bending becomes more pronounced. This problem does not occur in a notched tensile test such as the SENT test. Another advantage of this test is that the SENT test is instrumented and that force and displacement are recorded before and after crack initiation. The results of this test are discussed below.

SENT test

Specimens with different notch-tip radii were tested in a single-edge notch tensile test at 1 m/s clamp displacement. This resulted in an apparent macroscopic strain rate of 28.6 s^{-1}, calculated with the clamping distance at $t = t_0$. (Localization effects are ignored in this definition.) It should be noted that the strain rate of the material behind the notch tip could increase to 5000 s^{-1} because of strong localization of the deformation processes.[22] When the process zone has a size of 1 mm thickness the local strain rate already reaches 1000 s^{-1}.

The maximum stress during the fracture process is shown in Figure 10. The general trend observed from Figure 10 is that the maximum stress decreases gradually with temperature for all notch-tip radii. The fracture strength does not strongly depend on the stress concentration in this temperature range. Especially at higher temperatures the influence of the notch tip diminishes. This is attributed to the lowered yield stress at elevated temperatures. Yielding becomes more pronounced and this diminishes the differences in initial notch-tip radius. The maximum stresses do not convey to a single line at high temperatures, which

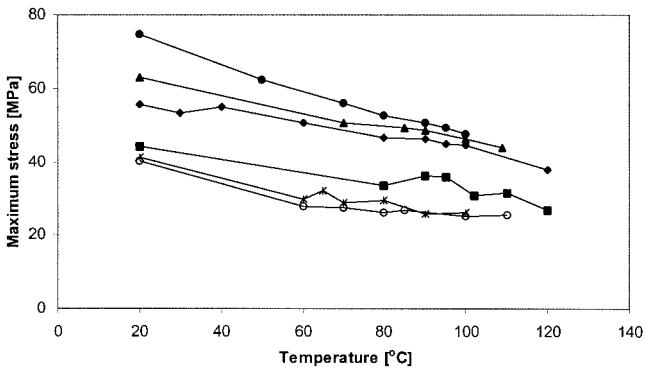

Figure 10 Maximum stress for different notch-tip radii as a function of temperature, PK–polymer, SENT, 28.6 s^{-1}. Notch-tip radius: ○, 2 μm; *, 15 μm; ■, 100 μm; ◆, 250 μm; ▲, 500 μm; ●, 1000 μm.

suggests that even in the ductile fracture mode, the notch-tip radius has an effect.

The maximum stress is plotted as a function of notch-tip radius at room temperature (Fig. 11). It is clear that the stress concentrations are different for different notches but the effect is negligible compared to the theoretical estimations.

The theoretical stress concentrations belonging to the different notch-tip radii are: $K_{tn} = 1.94$ with radius 1.0 mm; $K_{tn} = 2.56$, radius 0.5 mm; $K_{tn} = 3.34$, radius 0.25 mm. The smaller notch-tip radii have stress concentrations even larger than this, becoming infinite for the smallest radius. The experimental stresses, however, seem to be higher than expected from theory, indicating that blunting plays an important role in this polymer. Apparently, in this temperature range, the initial notch is deformed before a crack is initiated. This gives rise to a lower stress concentration behind the notch, and the critical macroscopic stress required for crack initiation will consequently be higher. The effect of notch-tip radius on the fracture strength is therefore reduced.

Particularly at sharp notches (sharper than 100 μm) the fracture stress does not decrease with notch-tip radius (Fig. 11). In this notch-tip regime the influence of stress concentrations is predicted to be strong. This indicates that a lot of local plastic deformation occurs in these fractures, although the macroscopic fracture is very brittle, but also that the blunting is not independent of notch radius.

The SENT curves are separated into two processes: energy absorption before crack initiation and energy absorption during crack propagation. The energy is integrated from the force–displacement curves; therefore the crack initiation displacement, crack propagation displacement, and the fracture energy are shown in Figure 12. In this study the fracture is considered to be ductile when additional energy has to be supplied to the system to propagate a crack.

Crack initiation

The crack initiation displacements increase with temperature. This increase with temperature is less strong for the sharper notches [Fig. 12(a)]. The two larger notch-tip radii (1000 and 500 μm) show a strong increase in crack initiation displacement in the ductile region. This enhanced increase is absent with the sharper notch-tip radii. With increasing notch-tip radius the amount of strain required to initiate a crack is increased. A larger notch-tip radius leads toward a larger resistance against crack formation. The strain necessary to form a crack in the polymer is increased with a larger notch-tip radius.

Crack propagation

The crack propagation displacements show the same dependency on temperature for all notch-tip radii

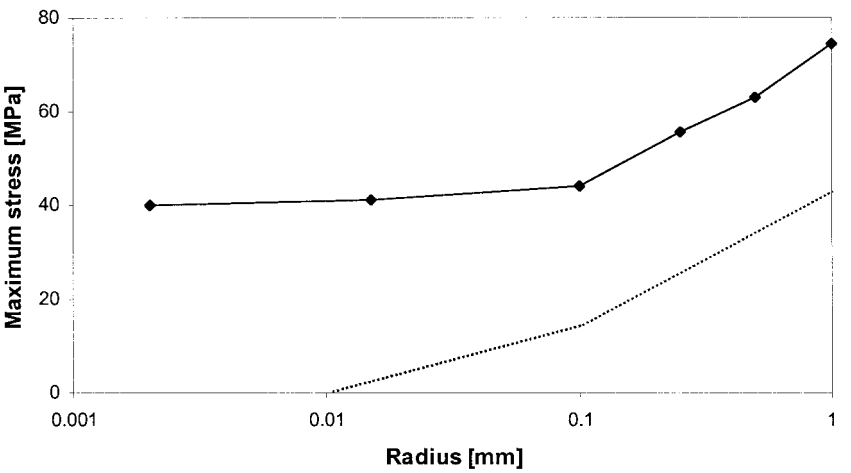

Figure 11 Maximum stress as a function of notch-tip radius for PK in SENT, 20°C, 28.6 s^{-1}; ◆, experimental data. Dotted line represents theoretical values from unnotched data and Figure 1.

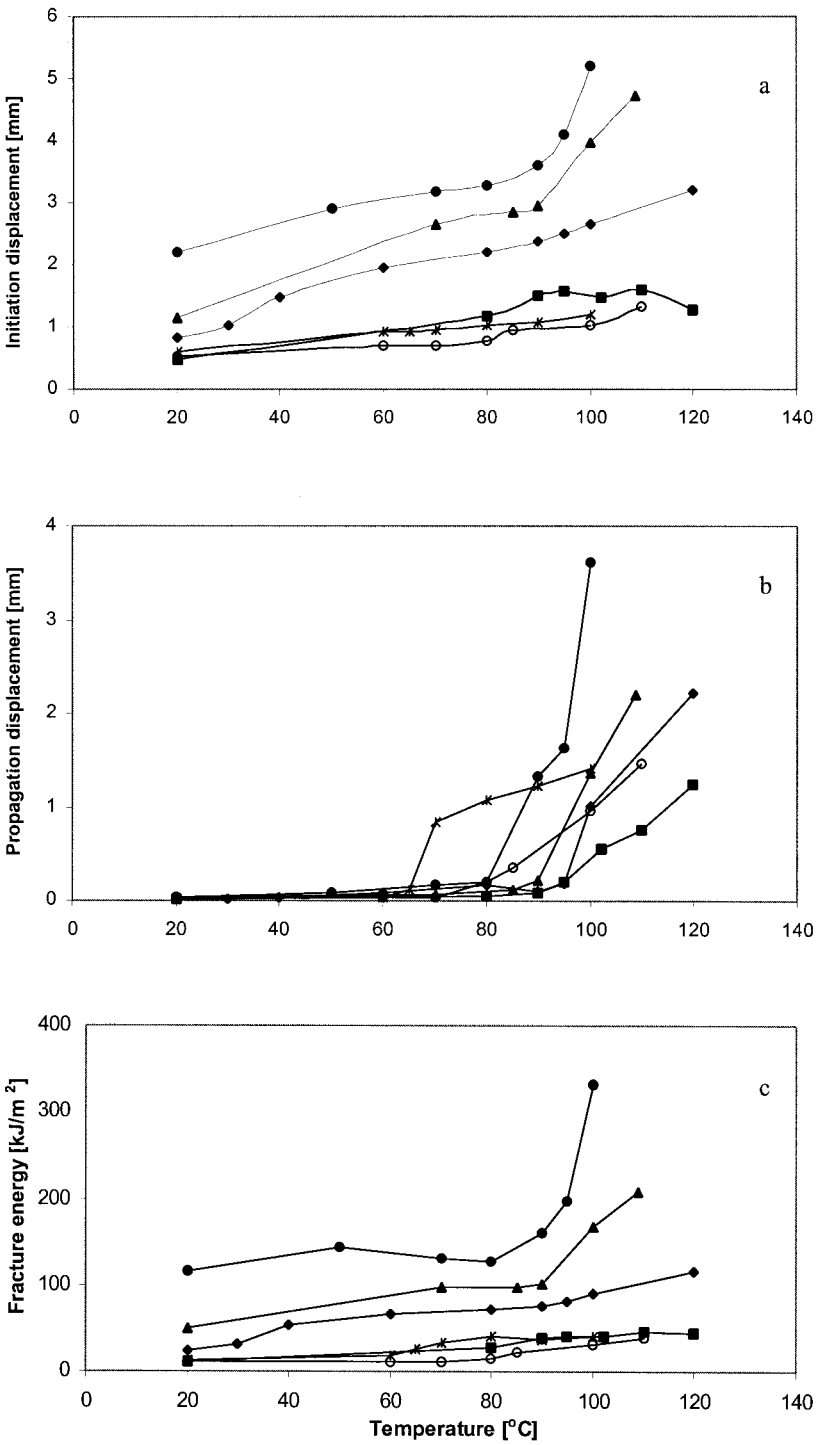

Figure 12 Initiation and propagation displacement and fracture energy as a function of temperature for different notch-tip radii, PK, SENT, 1 m/s (28.6 s^{-1}): ○, 2 μm; *, 15 μm; ■, 100 μm; ◆, 250 μm; ▲,500 μm; ●, 1000 μm.

[Fig. 12(b)]. At low temperatures the crack propagation displacement is close to zero. At a certain temperature the crack propagation displacement starts to increase steeply with temperature. This is attributed to the onset of ductility of the fracture. More energy needs to be supplied to the system to propagate a crack in this temperature range. The influence of a larger notch-tip radius on the crack propagation displacement is to lower the temperature where the onset of ductility occurs. It is seen in Figure 12(b) that for the two sharpest notch-tip radii, this is not the case. They both show a brittle-to-ductile transition at a lower temperature than expected. The crack propagation energy in the ductile region seems to be dependent on

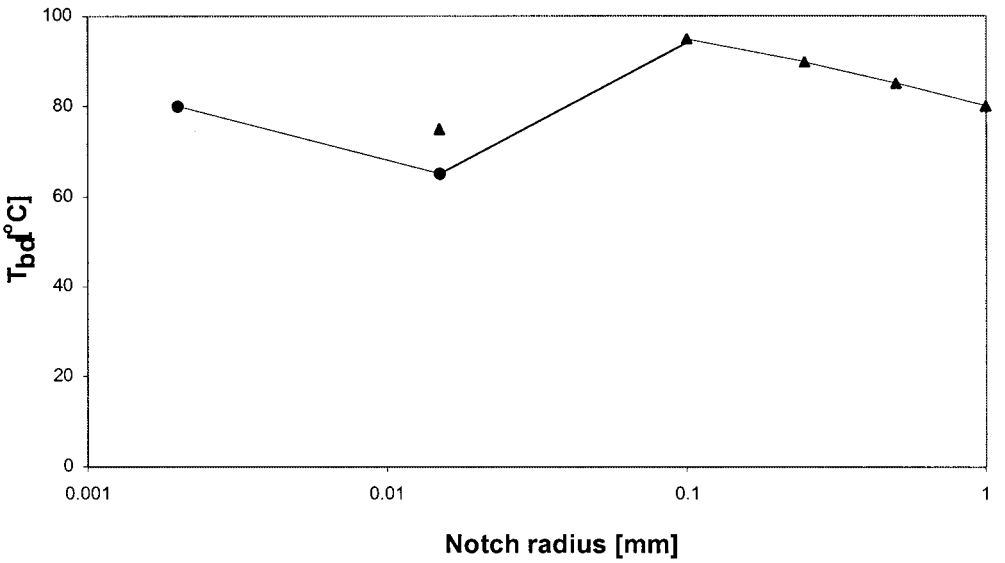

Figure 13 Brittle-to-ductile transition temperatures as a function of notch-tip radius, PK, SENT, 28.6 s^{-1}: ▲, produced with cutting technique; ●, laser-notched samples.

the notch-tip radius. The crack propagation consumes more energy with a larger initial notch-tip radius. Because a propagating crack always has the same tip radius, these differences must be attributed to the local plastic processes before crack initiation.

Fracture energy

Generally the fracture energy rises with temperature for all notch-tip radii [Fig. 12(c)]. The two largest notch-tip radii (1 and 0.5 mm) show a strong increase in fracture energy in the ductile regime. This stems mainly from the enhanced plasticity before crack initiation. The fracture energy is strongly dependent on the notch-tip radius. A larger notch-tip radius results in increased fracture energy, which has to do with the more severe localization effects when a sharper notch is present. When a smaller amount of material is involved, the consumption of energy during crack propagation and crack initiation are consequently lower.

Brittle-to-ductile transition

The onset of additional energy to propagate a crack is taken as a marker for ductility. The brittle-to-ductile transition temperature is taken at the point of onset of propagation displacement and energy. These T_{bd} values are plotted in Figure 13 as a function of notch-tip radius. The two sharpest notches show a decreased brittle-to-ductile transition temperature. Because these notches were produced with the laser technique and not milled into the specimen, a dependency on notching method was expected. To validate this hypothesis a series has been produced with a radius of 15 μm by means of a cutting technique. The result is also plotted in Figure 13. The notching method did not introduce a difference in behavior of the 15-μm radius notched series. The SENT data were similar for both series.

Moving from a notch-tip radius of 1 mm down to a notch radius of 0.1 mm the T_{bd} is increased. When the notch-tip radius is reduced further (from 0.1 to 0.015 mm) the T_{bd} is lowered and with the sharpest notches the T_{bd} starts to increase again. This anomalous effect of the two sharpest notches was also reported elsewhere.[12,13] This phenomenon can perhaps be explained by considering the driving forces for crack growth. A sharp notch has a higher stress concentration at the tip of the notch; consequently the crack initiation occurs at a lower macroscopic stress. This suggests that the notch tip is partially blunted. The result of this is that the amount of stored elastic energy at the moment of crack initiation in the whole sample is lower for a sharp notch than that for a blunted one. The driving force for crack growth is the release rate of the stored elastic energy. Obviously when less energy is available, the driving force for crack growth is smaller. A blunted notch can produce an instability during crack propagation. When the amount of elastic energy exceeds the energy absorption for surface creation the propagating crack is said to be unstable.[8] The crack speed in that case increases during crack propagation. This leads to the conclusion that a larger notch-tip radius is, although more blunted, more prone to produce instability, unless the material's resistance to crack growth is sufficient to ensure stable crack propagation.

The fracture surfaces of the larger notch-tip radii show a temperature range with mixed-mode fracture

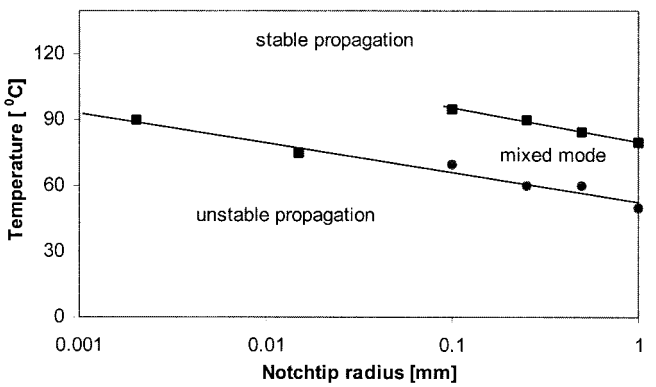

Figure 14 Onset of ductility as a function of notch-tip radius, PK, SENT, 28.6 s^{-1}: ■, ductility based on propagation data; ●, ductility based on fracture surfaces.

behavior: a local ductile zone behind the notch tip, followed by a brittle zone. The sharp notches do not show this mixed-mode fracture behavior. In Figure 14 the onset of this mixed-mode fracture behavior is plotted as a function of notch-tip radius. It appears that the onset of the mixed-mode behavior coincides with the line of stable propagation for the sharper notches. The brittle-to-ductile transition is delayed for the larger notch-tip radii because of the mixed-mode instability. It is suggested that two fracture mechanisms are operative: (1) a mechanism where the fracture changes from brittle to ductile without an instability occurring and (2) a mechanism where the fracture changes from brittle to a semiductile fracture with instable crack propagation and then finally to full ductile behavior with stable crack propagation at higher temperatures.

In addition to the evidence found for an instability phenomenon the complete records of force versus displacement are given (Fig. 15). The large notch-tip radii show some plastic behavior before crack initiation. This viscoplasticity was related to the "change of slope" before reaching the maximum force. The curves shown are all taken from the 80°C measurements. This is just around the T_{bd} for all notches. The two smallest notch-tip radii, which did not show an unstable crack propagation, show straight upgoing curves followed by either brittle or ductile crack propagation. The mixed-mode fracture was not encountered. The forces for the sharp notch tips are below the point of the hardening behavior shown for the larger notch-tip radii. This also indicates that the blunting of a notch can lead to an unstable crack propagation if the elastic energy release is large enough.[12,13,25]

Elastic stored energy

The anomalous behavior between the notch-tip radius of 0.1 and 0.015 mm (Fig. 15) could possibly be related to the amount of elastic energy stored in the sample. Aliphatic polyketones are known to store a lot of elastic energy upon loading compared with other polymers. This is illustrated in Figure 16. The yield point of aliphatic polyketones is situated at a high stress and combined with an unusual high yield

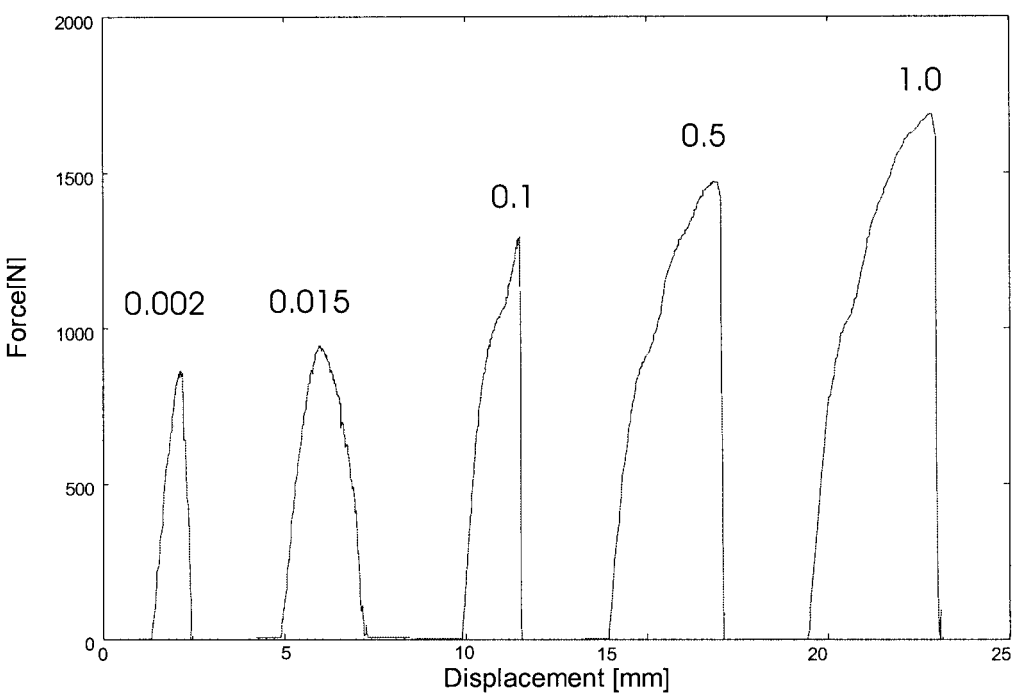

Figure 15 Force–displacement curves at 80°C for different notch-tip radii, PK, SENT, 28.6 s^{-1}.

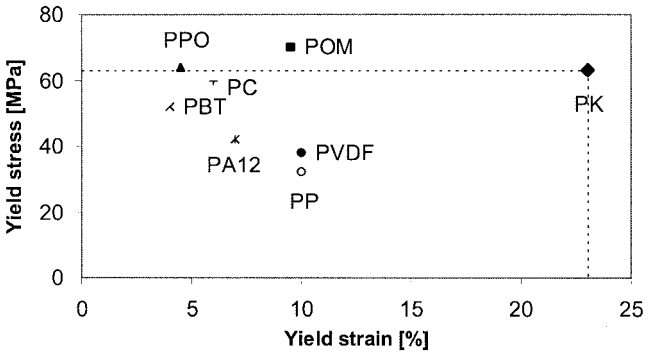

Figure 16 Yield point data for different polymers.

strain. The elastic energy stored during loading will therefore be considerably higher compared to that of other polymers.

To gain more insight in the behavior of the polymer in terms of crack propagation and driving force for crack propagation, the specimen length was reduced. A longer specimen can store more elastic energy before crack initiation occurs.[13,14,25] Changing the specimen length is a convenient method to study the effect of driving force for crack growth. The material resistance toward crack growth can be kept constant by keeping the same notch-tip radius—the localization effects will be equal. The piston speed was adjusted to maintain the same apparent macroscopic strain rate (based on clamping distance). The notch-tip radius of 0.1 mm was used, whereas the clamping length was reduced from 34 to 20 mm. The piston speed was reduced from 1 to 0.588 m/s. The elastic stored energy is reduced in this manner, by decreasing the amount of material where elastic energy can be stored. The results are shown in Figure 17.

The maximum stress in the SENT test remained constant; the stress was independent of specimen length. This is a logical response, given that the stress concentration factor is the same and the area behind the notch is kept constant; however, the initiation energy shows a difference. The specimen with reduced length consumes lower amounts of energy before a crack is initiated. The propagation displacement shows a substantial influence of specimen length. The shorter specimens show an earlier onset of ductility compared to the original specimen length. The transition of brittle to ductile is shifted to a lower temperature for the samples with reduced specimen length. The change of T_{bd} is about 25°C.

This illustrates that the balance of stored elastic energy and the resistance to crack growth determines whether the crack propagation is stable or instable, although this transition is not really discontinuous. The elastic energy storage is constantly decreasing upon decreasing clamping length. It is shown that making a notch sharper does not mean that the fracture will become more brittle; the amount of energy, however, decreases significantly with notch-tip radius because of localization effects.

Polyketone–rubber blends

The notch sensitivity of the PK terpolymer is a consequence of the localization of the deformation behind the notch tip. A well-known method to reduce the notch sensitivity of a polymer is the addition of a second elastomeric phase. The cavitation of this dispersed rubber phase delocalizes the deformation and as more material is deforming more energy is absorbed during fracture. A 10% CSR-phase was mixed into the polyketone polymer and samples were produced with notch-tip radii of 1, 0.5, 0.25, and 0.1 mm, and 2 μm, using the same techniques as with the polyketone terpolymer itself.

SENT test

The polyketone–10%CSR blend was also evaluated with the SENT test. Specimens were produced with different notch-tip radii ranging from 1 mm radius to 2 μm radius. The maximum stress measured during the fracture process is plotted as a function of temperature in Figure 18.

The stress level decreased gradually with temperature for all notch-tip radii. In the ductile region the stress levels converge on each other, indicating that notch-tip blunting is occurring at the notch tip. Although the rubber phase is present the different notch radii still show different maximum stresses. A larger notch-tip radius results in a higher stress level. Apparently in the ductile region blunting of a sharp notch is not complete.

The stress levels are somewhat higher than those for the polyketone polymer itself (Fig. 19). This is an indication that the cavitation of the rubber phase relieves some of the constraint ahead of the notch and more blunting is taking place. The sharpest notch shows a much higher stress than expected. The stress concentration calculated from theory predicts stress levels that converge to zero for such a notch. The theory assumes linear elastic behavior, which is clearly not valid for this material. It seems that when a notch is produced with a radius < 100 μm, the stress levels do not decrease. The same trend is observed for the notched Izod impact energy of PK shown in Figure 9.

The displacement and energy data show exactly the same trend; therefore only the initiation displacement and propagation displacement are given here, as well as the fracture energy (Fig. 20).

Crack initiation

The initiation displacements increase with temperature as expected [Fig. 20(a)]. At elevated temperatures

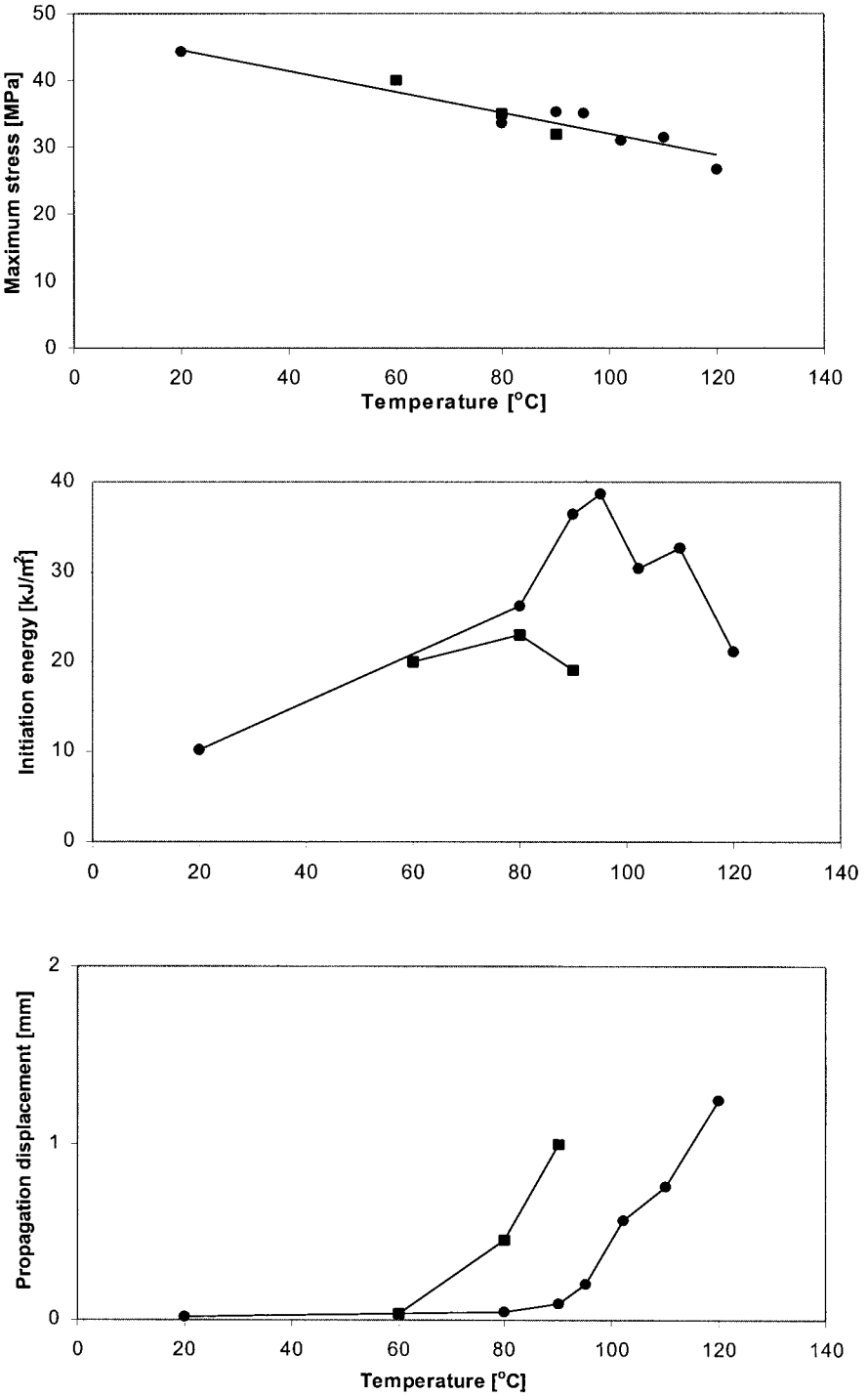

Figure 17 Maximum stress, initiation energy, and propagation displacement as a function of temperature, PK, SENT, 28.6 s^{-1}: ●, normal specimen length; ■, reduced specimen length.

the mobility of the polymer chains is higher. At higher temperatures therefore it is more difficult to introduce a crack in the polymer system. The influence of notch-tip radius is to increase crack initiation displacement. The process zone was also found to be larger with a larger notch-tip radius. The two sharpest notches show almost identical displacement and energy curves. This was also shown for the PK system and was related to the blunting of the notch before crack initiation occurs.

The crack initiation process is sometimes the dominating step in the fracture process, although this is not always necessary. The radius of a running crack is of the same magnitude, and the propagation of this crack can therefore be independent of the crack initiation process. For the polyketone homopolymer it was

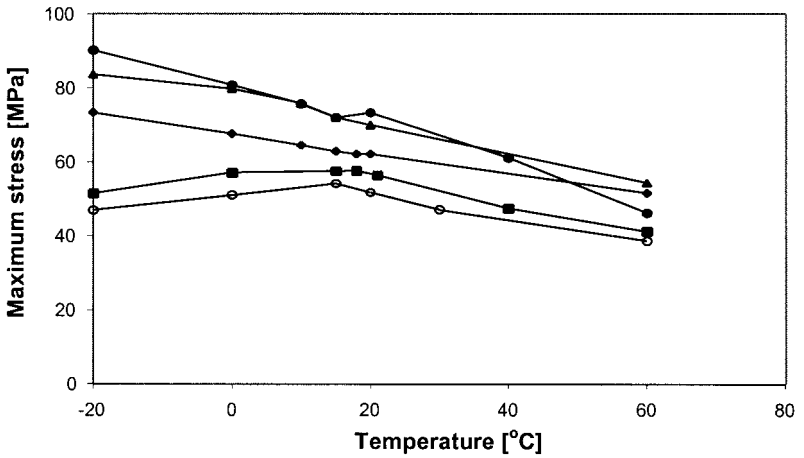

Figure 18 Maximum stress in SENT as a function of temperature for PK–CSR blend (apparent strain rate 28.4 s^{-1}): ○, 2 μm; ■, 100 μm; ◆, 250 μm; ▲, 500 μm; ●, 1000 μm.

shown that it is the competition between elastic energy release and plastic deformation of the polymer that determines whether the crack propagation is dependent on the initiation process. When the storage of elastic energy becomes larger the material will respond with greater brittleness during the crack propagation process. On the other hand more plastic deformation before crack initiation results in a more ductile response of the polymer. When the resistance versus crack propagation of the material is large (in the case of the blend), the initiation process is not important; only when the balance becomes critical the elastic energy may be decisive and the propagation becomes unstable (in the case of PK terpolymer).

Crack propagation

The crack propagation displacements show the same dependency on temperature for all notch-tip radii [Fig. 20(b)]. At low temperatures the displacement necessary to propagate a crack is close to zero. At a certain temperature the crack propagation displacement starts to rise steeply with temperature. This is attributed to the onset of ductility of the fracture. More energy needs to be supplied to the system to propagate a crack in this temperature range. The crack propagation measurements show that the onset of ductile behavior starts at about the same temperature for all notch-tip radii. This indicates that the notch-tip sensitivity is strongly reduced with the addition of a small volume of a cavitating rubber phase. Although the maximum stress and the resistance versus crack initiation are dependent on notch radius for the blend, the crack propagation clearly is not. The deformation is spread out over a larger part of the test specimen and therefore the notch-tip sensitivity is significantly reduced. The elastic instability effect found for the PK–polymer does not play a significant role for the blend, indicating a larger resistance toward crack growth.

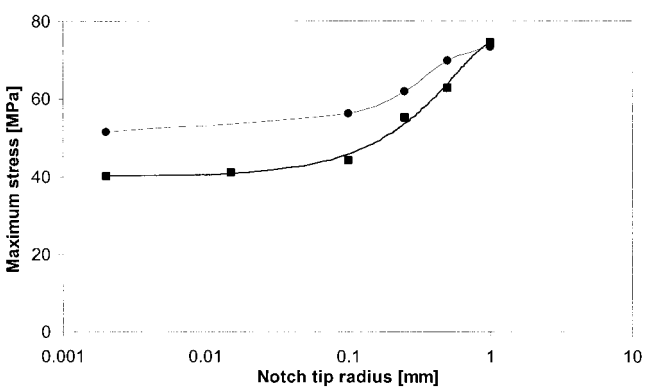

Figure 19 Maximum stress as a function of notch-tip radius, SENT, 28.6 s^{-1}: ●, PK–10%CSR blend; ■, PK.

Fracture process

The fracture energy increases with increasing temperature for all notch-tip geometries [Fig. 20(c)]. The transition from brittle to ductile fracture is clearly visible in the fracture energy, which differs from the PK polymer itself. The total fracture energy shows an increase with increasing notch-tip radius, which is attributed to the crack initiation process. It can be concluded that a larger notch-tip radius does not lead to a lowering of the brittle-to-ductile transition temperature in the PK_{90}–CSR_{10} blend, but it leads to an increase in impact energy by the increased resistance versus crack initiation. This is a remarkable difference with the polyketone homopolymer where the T_{bd} is sensitive to changes in notch-tip radius.

Brittle-to-ductile transition

The fracture mechanism of rubber cavitation followed by shear yielding of the matrix polymer suppresses

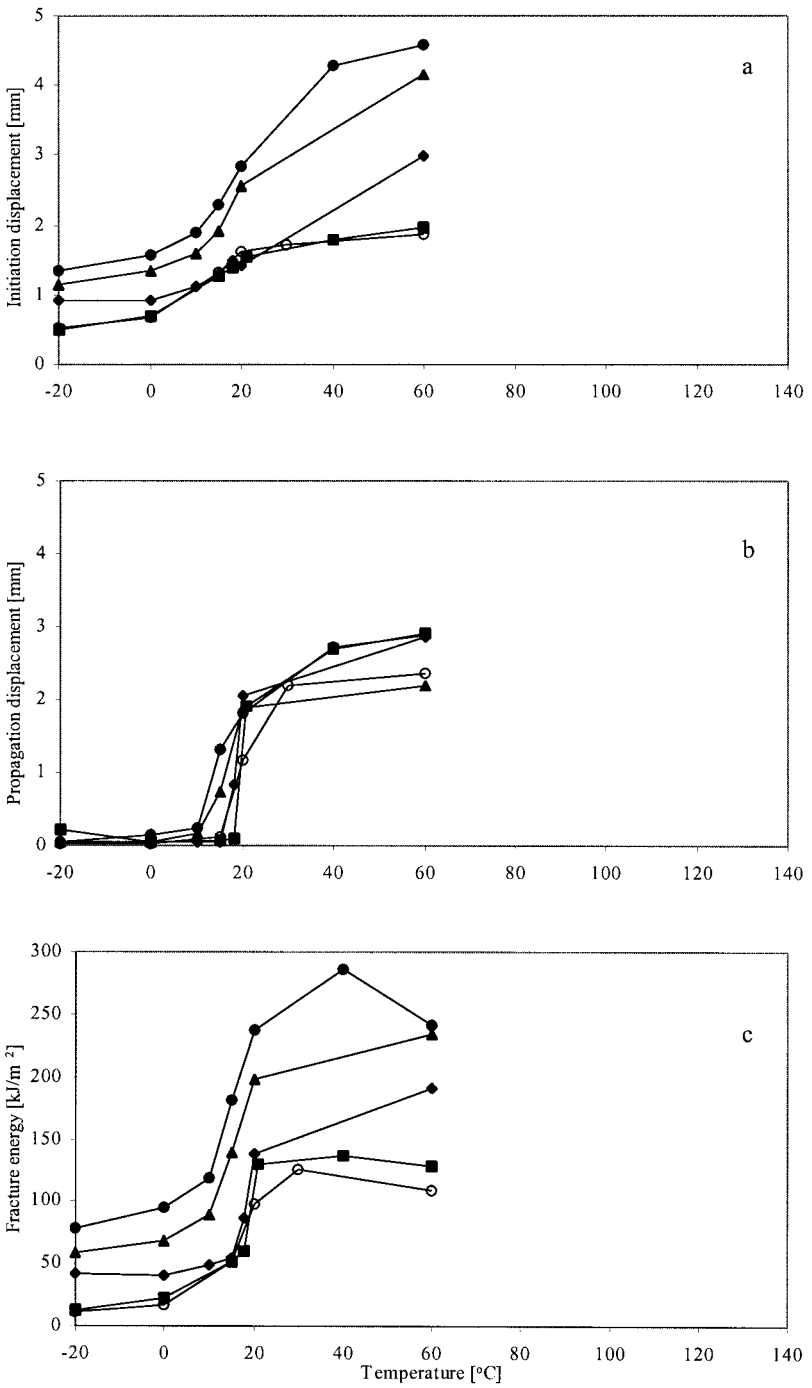

Figure 20 Initiation and propagation displacement and fracture energy versus temperature for PK–CSR blend: ○, 2 μm; ■, 100 μm; ◆, 250 μm; ▲, 500 μm; ●, 1000 μm.

crazing of the matrix polymer. This leads to a reduced sensitivity toward stress concentration behind the notch tip and enables the polymer to plastically deform during the fracture process. This is illustrated in Figure 21.

The T_{bd} of the polyketone terpolymer becomes almost independent of notch-tip radius with the addition of 10% of a soft elastomeric phase. The toughening effect of this core–shell rubber is substantial. Only a small amount of rubber phase is needed to stabilize the notch-tip sensitivity.

Infrared thermography

Temperature at the surface of the specimen was monitored during fracture, using an infrared (IR) camera, producing 30 frames/s. During fracture localized viscoelastic and plastic energy dissipative processes oc-

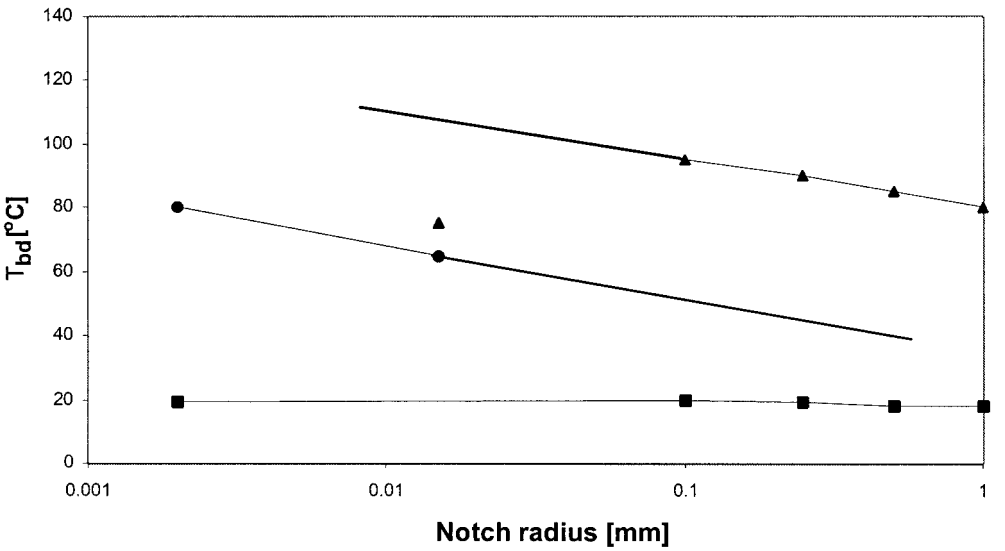

Figure 21 Brittle-to-ductile transition temperatures as a function of notch-tip radius, SENT, 28.6 s^{-1}: ▲, PK (milled notches); ●, PK (laser notches); ■, PK–10%CSR blend.

cur in the vicinity of the crack tip. These processes are responsible for the energy absorption in the material. At adiabatic conditions these dissipative processes can be attributed to a significant temperature rise of the process zone. The fracture process will then develop in a more localized manner as a consequence of softening of the material. The frames shown were taken just before crack initiation occurred.

A zone with increased temperature was visible ahead of the notch, where large plastic deformation occurred (Fig. 22). This zone was thicker in the case of a larger notch. Extreme blunting occurred, especially in the 1-mm notch, and the radius of the notch visibly increased during testing. The highest temperature in the deformation process zone was located at some distance ahead of the notch tip or the running crack.

The thickness of the temperature zone increased with notch-tip radius. This increase in zone size indicated that the deformation process develops more locally when a sharp notch is present in the specimen. The increase also corresponds to the influence of notch radius on initiation displacement, which showed an increase with increasing notch radius.

A running crack in a 1-mm notched sample is shown in Figure 23. The sample was deformed in the SENT setup at a low piston speed of 10^{-4} m/s. The original notch-tip radius is deformed to a large extent before crack initiation sets in. Local shear yielding blunts the notch and enhances the resistance toward crack initiation. When a crack is initiated, the crack propagation is initially very fast and then slows down during propagation. The crack propagation stabilizes during the propagation process; the temperature behind the notch is lowered when the crack advances through the ligament. This is an indication that the local strain rate decreases when the crack propagates through the ligament. The first stage of crack propa-

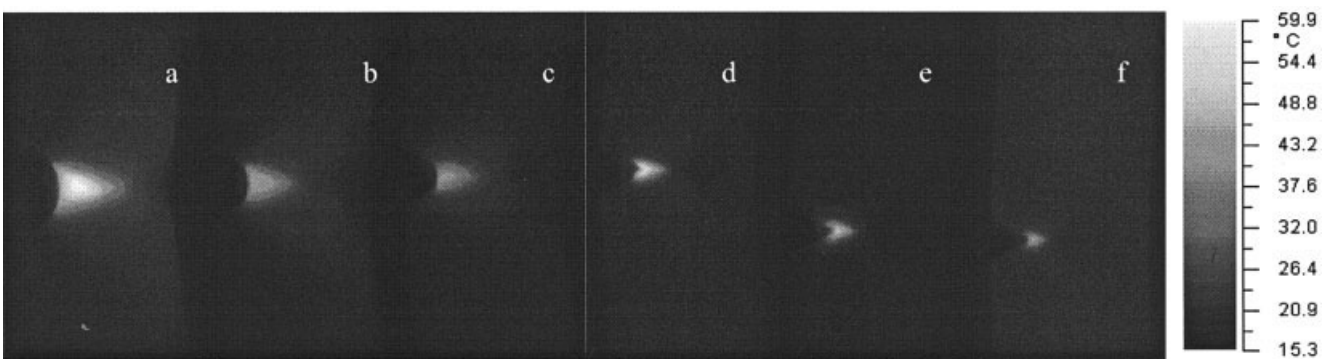

Figure 22 Process zones just before crack initiation at 1×10^{-3} m/s (2.86×10^{-2} s^{-1}): (a) 1 mm, (b) 0.5 mm, (c) 0.25 mm, (d) 0.1 mm, (e) 0.015 mm, (f) 0.002 mm.

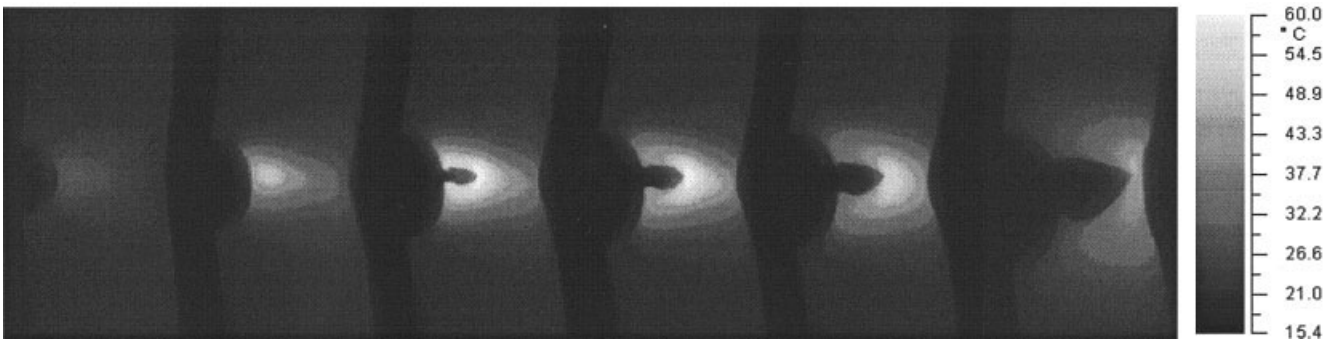

Figure 23 Running crack in PK polymer, 1-mm notch-tip radius, SENT, 10^{-4} m/s (2.86×10^{-3}).

gation is enhanced by the elastic strain release of the whole sample.

CONCLUSIONS

The fracture behavior of the PK–terpolymer is sensitive toward changes in notch-tip radius. The fracture energy decreases strongly with decreasing notch-tip radius even when fractured ductile. Sharper notches were not as effectively blunted as were the larger notches in the ductile region. The T_{bd} was increased with decreasing notch-tip radius for the larger notches (1000–100 μm). For sharper notches (2 and 15 μm) the T_{bd} decreased again. This behavior could be explained by the decreasing amount of elastic energy release with sharper notches. The energy release proved to be very important for this material. A mixed-mode fracture behavior was found to occur with larger notches because of the elastic energy present in the sample before fracture. The notch sensitivity was reduced considerably by the addition of a 10% core–shell rubber phase. Notch-tip radius for the blend material showed almost no effect on the T_{bd}. The fracture energy on the other hand was still lowered with a sharper notch. This was attributed to the difference in the crack initiation process.

References

1. Kinloch, A. J. Met Sci 1980, 14, 305.
2. Brown, H. R. J Mater Sci 1982, 17, 469.
3. van der Wal, A.; Gaymans, R. J. Polymer 1999, 40, 6045.
4. Dijkstra, K.; van der Wal, A.; Gaymans, R. J. J Mater Sci 1994, 29, 3489.
5. Pitman, G. L.; Ward, I. M. Polymer 1979, 20, 895.
6. Chang, F. C.; Hsu, H. C. J Appl Polym Sci 1994, 52, 189.
7. Ward, I. D. Mechanical Properties of Solid Polymers; Wiley: London, 1971.
8. Chang, F. C.; Chu, L. H. J Appl Polym Sci 1992, 44, 1615.
9. Gaymans, R. J.; Hamberg, M. J. J.; Inberg, J. P. F. Polym Eng Sci 2000, 40, 256.
10. Vincent, P. I. Impact Test and Service Performance of Thermoplastics; Plastics Institute: London, 1971.
11. Gaymans, R. J. Polymer Blends; Wiley: New York, 2000; Chapter 25.
12. Kinloch, A. J.; Young, R. J. Fracture Behavior of Polymers; Applied Science: London, 1983.
13. Dekkers, M. E. J.; Hobbs, S. Y. Polym Eng Sci 1987, 27, 1164.
14. Williams, J. G. Fracture Mechanics of Polymers; Wiley: New York, 1987.
15. Pilkey, W. D.; Peterson, R. E. Peterson's Stress Concentration Factors; Wiley: New York, 1974.
16. Bucknall, C. B. Polymer Blends; Wiley: New York, 2000; Chapter 21.
17. Plati, E.; Williams, J. G. Polym Eng Sci 1975, 15, 470.
18. Kinloch, A. J.; Shaw, S. J.; Hunson, D. L. Polymer 1983, 24, 1355.
19. Fraser, R. A. W.; Ward, I. M. J Mater Sci 1977, 12, 459.
20. Havriliak, S., Jr.; Cruz, C. A., Jr.; Slavin, S. E. Polym Eng Sci 1996, 36, 2327.
21. Polato, F. J Mater Sci 1985, 20, 1455.
22. Furno, F. J.; Webb, R. S.; Cook, N. P. J Appl Polym Sci 1964, 8, 101.
23. Gaymans, R. J.; Borggreve, R. J. M. Contemporary Topics in Polymer Science, 6th ed.; Culbertson, B. M., Ed.; Plenum Publishers: New York, 1989; p 46.
24. Béguelin, P.; Barbezat, M.; Kausch, H. H. J Phys III France 1991, 1, 1867.
25. Fineberg, J.; Gross, S. P.; Marder, M.; Swinney, H. L. Phys Rev B 1992, 45, 5146.